Suplemento de la Revista Mexicana de Física **4** 021114 (2023) 1–6

Electromagnetic time-like form factors

Ángel S. Miramontes

Instituto de Física y Matemáticas, Universidad Michoacana de San Nicolás de Hidalgo, Morelia, Michoacán 58040, Mexico.

Adnan Bashir

Instituto de Física y Matemáticas, Universidad Michoacana de San Nicolás de Hidalgo, Morelia, Michoacán 58040, Mexico.
Theory Center, Jefferson Lab, Newport News, VA 23606, USA.

Received 20 May 2023; accepted 20 April 2023

We present the calculation of charged pion and kaon electromagnetic form factors in the time-like regime using Schwinger-Dyson equations and the Poincaré covariant Bethe-Salpeter equations within an SU(2) isospin symmetric limit. To accurately represent the behavior of a time-like photon, we have incorporated non-valence contributions into the system of equations, enabling the decays $\rho \to \pi\pi$ and $\phi \to KK$. The inclusion of these decay mechanisms is essential for capturing the expected behavior of the electromagnetic pion and kaon form factors. Our results for the form factors reasonably reproduce the experimental data for a time-like photon.

Keywords: Meson form factors; Schwinger-Dyson equations; Bethe-Salpeter equations.

DOI: https://doi.org/10.31349/SuplRevMexFis.4.021114

1. Introduction

Electromagnetic form factors of mesons such as pions and kaons are fundamental quantities that can be measured experimentally through elastic scattering or annihilation processes, and provide crucial information on the hadron structure. The study of form factors has been a subject of intense research for many decades, and has played a key role in our understanding of the strong interaction and its manifestation in the properties of hadrons.

The pion and kaon are of particular interest, as they are the lightest mesons and have the simplest quark content. They are also abundant in nature and can be produced in high-energy collisions, allowing for a wide range of experimental investigations. The electromagnetic form factors of the pion and kaon have been studied extensively using various experimental and theoretical methods. From the experimental side, the form factors have been measured with high precision for a space- and time-like photons [1–10]. From the phenomenological and theoretical side, there exist plenty of efforts to describe the form factor on the space-like regime (*i.e* [11–22] which are in agreement with the experimental determinations. Both the Electron-Ion Collider and the Jefferson Laboratory (current 12 GeV and potential 22 GeV upgrade) plan to chart out a large momentum range of space-like pion and kaon form factors.

In the time-like region, however, the situation is more complex and limited research is available, for example in dispersion theory [23, 24], vector meson dominance models [25], Lattice QCD [26] and recently within Bethe-Salpeter equations (BSEs) [27, 28]. The form factor in this region is related to the cross section for $e + e$- annihilation into hadrons, and is an important quantity for testing the fundamental principles of QCD. Theoretical calculations of the time-like form factor are challenging, as they require non-perturbative methods that can account for the strong interaction between quarks and gluons. In recent years, there has been significant progress in the development of non-perturbative approaches to QCD, such as Schwinger-Dyson equations (SDEs) and BSEs, which provide a systematic and rigorous framework for the calculation of hadron properties. On one hand, the SDEs describe the behavior of Green functions of QCD, while the BSE is used to study the properties of hadrons, which are bound states of quarks [13, 29–35].

In this contribution, we employ the SDEs and BSEs to delve into the electromagnetic form factors of pions and kaons in the time-like region. Our primary goal is to offer an in-depth analysis of the form factor and its characteristics within this region, while contrasting our findings with experimental data. Our research seeks to incrementally improve the understanding of the internal structure of pions and kaons, and to offer valuable perspectives on the underlying concepts of QCD in the non-perturbative regime.

This contribution is organized as follows, in Sec. 2 we present a description of the formalism of the SDE/BSE approach, in Sec. 3 we describe how the electromagnetic form factors are extracted in this formalism and in Sec. 4 we show our results for the pion and kaon form factor. Finally, in Sec. 5 we present our conclusions.

2. Formalism

In this section we summarize the principal elements of the SDE/BSE formalism. For a more complete description we refer to [36, 37].

The SDE for the dressed quark propagator can be written as follows,

$$S^{-1} = S_0^{-1} - Z_{1f} \int_q \gamma_\mu S(q) \Gamma^{qgl}_\nu(q,k) D_{\mu\nu}(k) \,, \quad (1)$$

where $S_0^{-1}(p)$ corresponds to the renormalized bare quark propagator

$$S_0^{-1}(p) = Z_2 \left(i\not{p} + Z_m m \right) \,, \quad (2)$$

with Z_{1f}, Z_2 and Z_m are the renormalization constants associated with the quark-gluon vertex, the quark propagator and the quark mass, respectively. Additionally, m is the current quark mass, $D_{\mu\nu}$ is the full gluon propagator, and in the Landau gauge reads as,

$$D_{\mu\nu}(k) = \left(\delta_{\mu\nu} - \frac{k_\mu k_\nu}{k^2} \right) \frac{Z(k^2)}{k^2} \,, \quad (3)$$

with $Z(p^2)$ being the gluon dressing function and Γ^{qgl} is the full quark-gluon vertex. For the simplicity of notation, we have suppressed the color indices.

Conversely, the description of mesons as bound states consisting of a quark and an anti-quark can be achieved using the homogeneous BSE. This equation is expressed as follows:

$$(\Gamma)_{a\alpha,b\beta}(p,P) = \int_q K^{r\rho,s\sigma}_{a\alpha,b\beta}(P,p,q) \times S_{r\rho,e\epsilon}(k_1)(\Gamma)_{e\epsilon,n\nu}(q,P) S_{n\nu,s\sigma}(k_2), \quad (4)$$

where P is the total momentum of the meson. For pseudoscalar mesons, abbreviated as $_{PS}$ in the subscripts below, the Dirac part of the Bethe-Salpeter amplitude (BSA) can be expanded in a tensorial basis with four elements:

$$\Gamma^i_{PS}(p,P) = \tau^i \gamma_5 \{ E_{PS}(p,P) - i\not{P} F_{PS}(p,P) - i\not{p}(p\cdot P) G_{PS}(p,P) - \left[\not{P}, \not{p}\right] H_{PS}(p,P) \} \,. \quad (5)$$

Here, E_{PS}, F_{PS}, G_{PS} and H_{PS} are four independent dressing functions. The interaction kernel in Eq. (4) is represented by $[K(P,p,q)]$; it contains all possible interactions among quarks and gluons within the bound state.

Finally, the quark-photon vertex (QPV) serves as a crucial component in examining the electromagnetic interactions of hadrons. This vertex represents the connection between quarks and the electromagnetic field, playing a vital role in determining the electromagnetic form factors of hadrons. Within this framework, the QPV can be characterized by solving an inhomogeneous BSE:

$$(\Gamma^\mu)_{a\alpha,b\beta}(p,Q) = Z_2 \left(\gamma^\mu\right)_{ab} t_{\alpha\beta} + \int_q K^{r\rho,s\sigma}_{a\alpha,b\beta}(Q,p,q) \; S_{r\rho,e\epsilon}(k_1) \times \left(\Gamma^{i,\mu}\right)_{e\epsilon,n\nu}(Q,q) \, S_{n\nu,s\sigma}(k_2) \,. \quad (6)$$

In this equation, Z_2 represents a renormalization constant, and $S(k)$ is the fully dressed quark propagator. The photon momentum is denoted by Q, while p and q signify the external and internal relative momenta between the quark and the antiquark, respectively. The variables k_1 and k_2 are defined as $k_1 = q + Q/2$ and $k_2 = q - Q/2$, such that $Q = k_1 - k_2$ and $q = (k_1 + k_2)/2$. Latin letters indicate Dirac indices, whereas Greek letters represent flavor indices. The isospin structure of the vertex can be described by the following expression: $t_{\alpha\beta} = \mathrm{diag}\,(2/3, -1/3, -1/3)$. It is important to remark that the QPV can be decomposed in a basis composed of twelve elements, eight being transverse to the photon momentum and four non-transverse, all twelve elements are included in our calculations.

In practical calculations of observables using the coupled system of SDE/BSE, the expansion of the interaction kernel must be truncated to a sum of a finite number of terms. The truncation must be carefully selected to ensure that the relevant symmetries are preserved in the calculation. Generally, our goal is to choose a truncation that adheres to the Ward-Takahashi identities. On one hand, chiral physics will be accurately incorporated in the calculations if the truncation complies with the Axial-Vector Ward-Takashashi identity (AxWTI). On the other hand, satisfying the Vector Ward-Takahashi identity guarantees the proper implementation of charge conservation.

In this context, one of the simplest truncations that satisfies both Ward-Takahashi identities is the widely recognized Rainbow-Ladder truncation (RL), in which the interaction kernel and SDE for the quark propagator are simplified by a vector-vector gluon exchange. Under these conditions, the interaction kernel can be expressed as:

$$K^{r\rho,s\sigma}_{a\alpha,b\beta}(Q,p,q) = \alpha\left(k^2\right) \gamma^\mu_{ar} \gamma^\nu_{sb} D^{\mu\nu}(k) \, \delta^{\alpha\rho} \delta^{\sigma\beta} \,, \quad (7)$$

where $k = p - q$, the color indices were omitted. Furthermore, the truncated quark SDE in the RL truncation reads,

$$Z_{1f} \gamma_\mu Z(k^2) \Gamma^{\mathrm{qgl}}_\nu(q,p) \to Z_2^2 \gamma_\mu 4\pi\alpha(k^2) \gamma_\nu \,. \quad (8)$$

Here, $\alpha(k^2)$ is an effective coupling that provides strength to the quark-antiquark interaction. In this contribution, we employ the Maris-Tandy model (MT) to describe $\alpha(k^2)$. It reads as follows

$$\alpha(q^2) = \pi\eta^7 \left(\frac{q^2}{\Lambda^2}\right)^2 e^{-\eta^2 \frac{q^2}{\Lambda^2}} + \frac{2\pi\gamma_m \left(1 - e^{-q^2/\Lambda_t^2}\right)}{\ln[e^2 - 1 + (1 + q^2/\Lambda^2_{QCD})^2]} \,. \quad (9)$$

The first term consists of a Gaussian component that supplies sufficient interaction strength for dynamical chiral symmetry breaking to occur, while the second term reproduces the one-loop QCD behavior of the quark propagator at high momenta. The free parameters of the MT model, Λ and η, are adjusted to match the pion mass and its weak decay constant. Within the SDE/BSE framework, the running quark masses m_u, m_d, and m_s are also incorporated as input parameters.

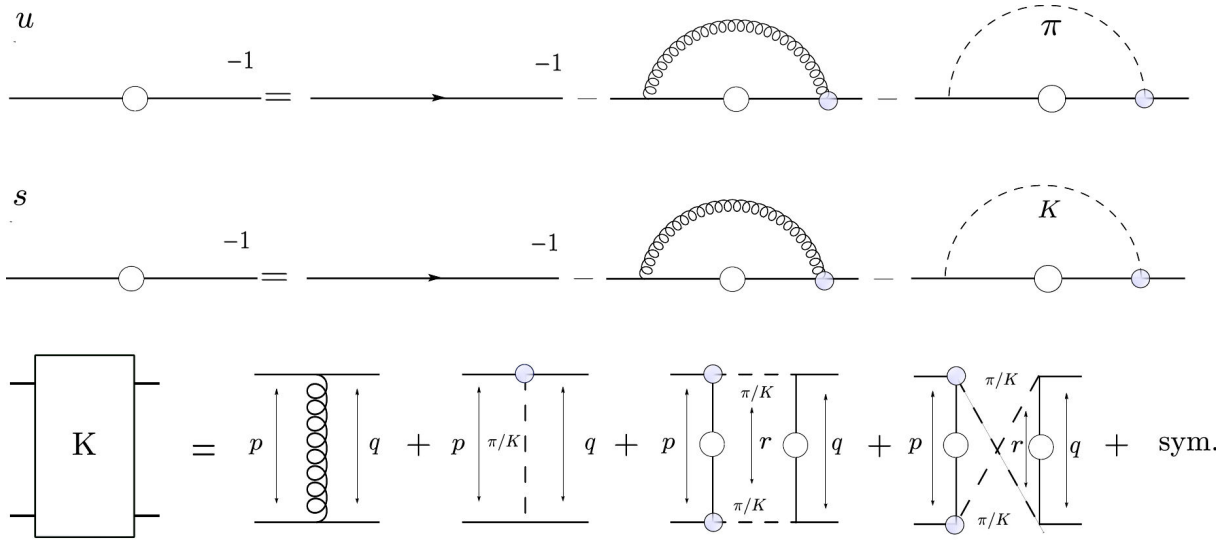

FIGURE 1. The truncations applied in this work for the BSE interaction kernel K (depicted in the lower diagram) and the quark SDE (shown in the upper diagram) are as follows: In the lower diagram, the components on the right-hand side represent the rainbow-ladder, t-channel pion/kaon exchange, and the s- and u-channel pion/kaon decay contributions to the truncation, respectively. It is important to note that the s- and u-channel pion/kaon decay elements do not have any impact on the quark SDE.

The scale $\Lambda_t = 1$ GeV is introduced solely for technical purposes and does not influence the calculated observables. The anomalous dimension is given by $\gamma_m = 12/(11N_c - 2N_f) = 12/25$, with $N_f = 4$ flavors and $N_c = 3$ colors. For the QCD mass scale, we adopt $\Lambda_{QCD} = 0.234$ GeV.

As extensively discussed in Refs. [27, 28, 38], the solutions of the BSE utilizing the RL truncation yield stable bound states, but they do not account for a decay mechanism for resonances. To accurately describe the QPV and, consequently, the hadronic form factors in the time-like regime, the decay mechanism of resonances must be incorporated. To achieve this, we employ a Beyond Rainbow-Ladder (BRL) truncation that introduces explicit mesonic contributions into the SDE/BSE system. A diagrammatic representation of this can be seen in Fig. 1, while the explicit integral expressions can be found in Ref. [38]. This type of truncation has been explored for investigating non-valence contributions to the quark propagator and hadronic masses [39–41]. Recently, the BRL truncation was used to describe the decay $\rho \to \pi\pi$ in [38, 42], resulting in a reasonable depiction of the pion and kaon electromagnetic time-like form factors [27, 28].

3. Electromagnetic form factor

The interaction of a virtual photon with a pseudoscalar meson M is described by a single form factor, $F_M(Q^2)$, and is conveniently written as:

$$\langle \mathbf{P}(p_1)|J^\mu|\mathbf{P}(p_2)\rangle = e(p_1+p_2)^\mu F_M(Q^2)\ , \qquad (10)$$

where we define Q as the total photon four-momentum, represented by $Q = p_1 - p_2$. The elementary electromagnetic charge is symbolized as e. Additionally, the electromagnetic current, which characterizes the interaction between a single photon and a quark-antiquark system reads,

$$J^\mu = \bar{\Psi}^f_{\mathbf{P}} G_0(\mathbf{\Gamma}^\mu - K^\mu) G_0 \Psi_{\mathbf{P}}{}^i\ , \qquad (11)$$

where $\Psi^i_{\mathbf{P}}$ and $\Psi^i_{\mathbf{P}}$ are the BSA of the incoming and outgoing meson M, respectively. The factor G_0 encapsulates the suitable multiplication of dressed quark propagators, while $\mathbf{\Gamma}^\mu$ symbolizes the diagrams following the impulse approximation (IA) approach, illustrating the interaction of photons

TABLE I. Numerical results for the masses and their respective decay constants. For BRL I we employ $\eta = 1.5$ and $\Lambda = 0.78$ GeV, and for BRL II $\eta = 1.6$ and $\Lambda = 0.74$ GeV. The masses M_ρ, M_ϕ and the respective decay widths have been extracted from our resulting time-like form factor using Pade approximant, while the masses m_ρ and m_ϕ have been computed only using RL and t-meson exchange diagrams (*i.e.*, no decay mechanism included). All mass-dimensioned quantities are expressed in GeV. The experimental values have been extracted from Ref. [43].

	BRL I	BRL II	Exp.
m_π	0.139	0.128	0.139
f_π	0.138	0.135	0.131
m_k	0.493	0.480	0.493
f_k	0.159	0.157	0.156
m_ρ	0.762	0.737	0.775
f_ρ	0.225	0.220	0.216
m_ϕ	1.077	1.036	1.019
f_ϕ	0.265	0.260	0.236
M_ρ	0.752	0.728	0.775
Γ_ρ	0.122	0.123	0.145
M_ϕ	1.077	1.030	1.019
Γ_ϕ	0.006	0.005	0.004

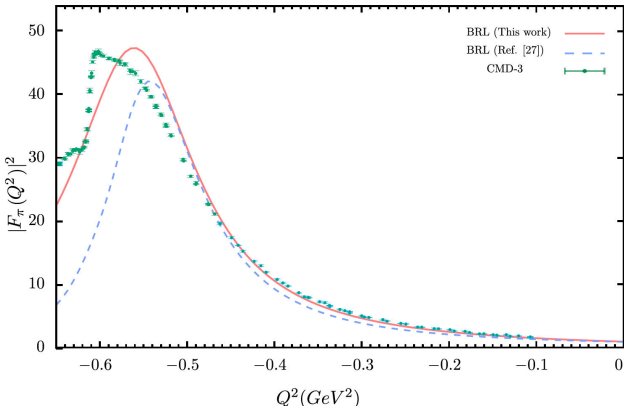

FIGURE 2. Absolute value squared of the electromagnetic pion form factor on the time-like $Q^2 < 0$ region compared with experimental data. We observe that including the full pion amplitude (solid line) into the interaction kernel leads to a better description of the form factor, compared with the previous calculation where only the leading γ_5 (dashed line) amplitude was employed [27,44]. The parameters used were $\eta = 1.5$ and $\Lambda = 0.78$. The experimental data was extracted from [45].

with the dressed valence quarks. It's important to note that, for the calculations showcased in this paper, we've considered solely the diagrams corresponding to the IA to simplify the numerical computations.

Upon acquiring the relevant quark propagators by solving their SDEs, determining the meson amplitudes through the solution of the homogeneous BSE, and obtaining the QPV by solving the inhomogeneous BSE, we can successfully extract the electromagnetic form factor.

4. Results

To compute the electromagnetic form factors, we have employed the BRL truncation with two distinct sets of free parameters in the MT interaction. For the first set (BRL I), we use $\eta = 1.5$ and $\Lambda = 0.78$, while for the second set (BRL II), we adopt $\eta = 1.6$ and $\Lambda = 0.74$. The first parameter set is utilized to calculate the electromagnetic pion form factor, whereas the second set is applied to compute the kaon form factor. Furthermore, in our calculations, we use the quark masses $m_q = 6.8$ MeV and $m_s = 85$ MeV at the renormalization scale $\mu = 19$ GeV. The values for the masses and decay constants can be found in Table I. Our results for the electromagnetic form factor of the charged pion are illustrated in Fig. 2. It is important to remark that the time-like electromagnetic pion form factor was earlier calculated in Ref. [27], where only the leading γ_5 pion amplitude was employed on the quark-pion vertices from Fig. 3. For this contribution, we have computed the form factor employing the four pion amplitudes, which leads to a better description on the time-like regime compared with the previous calculation in Ref. [27]. In a similar case, our result for the kaon form factor is displayed in Fig. 3, where also the four kaon amplitudes have been included in the quark-kaon vertex in Fig. 1. In both cases, our results using the BRL truncation exhibit a qualitatively accurate and quantitatively satisfactory behavior in comparison with the experimental data. It is important to note that such results cannot be achieved using only the RL truncation; it is the incorporation of the s- and u- meson exchange channels that enables the proper representation of the form factors. Lastly, the resonance pole positions (M_ρ, M_ϕ, and their corresponding decay widths) can be extracted by parametrizing the solutions with a Padé approximants fit and identifying the poles. From the first parameter set BRL I, the ρ resonance pole in the pion form factor is situated at $M_\rho = 0.752$ GeV and $\Gamma_\rho = 0.122$ GeV. Conversely, from the set BRL II, the ϕ resonance pole in the kaon form factor is located at $M_\phi = 1.030$ GeV and $\Gamma_\phi = 0.005$ GeV.

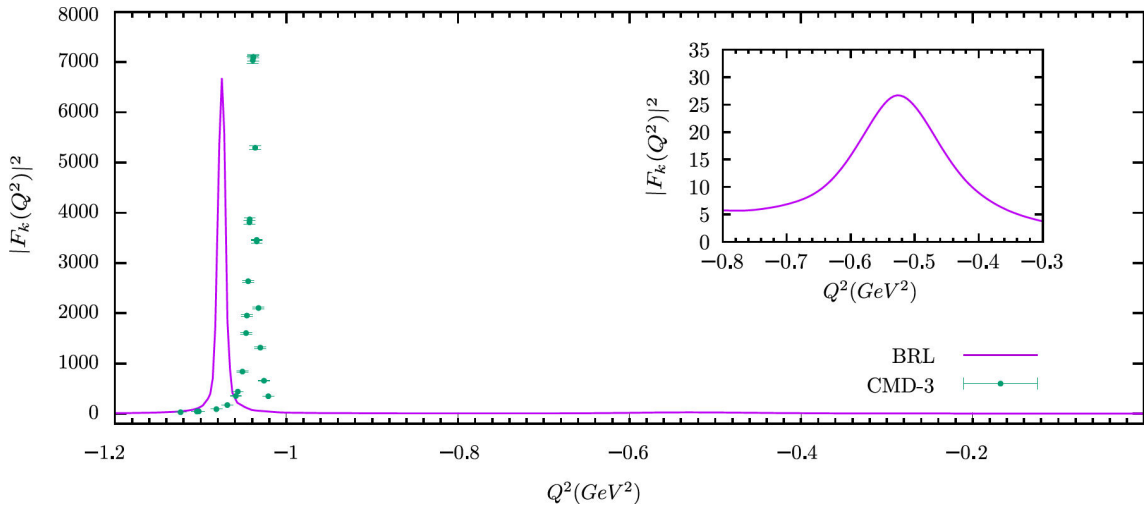

FIGURE 3. Absolute value squared of the electromagnetic kaon form factor on the time-like $Q^2 < 0$ region. We use the parameters $\eta = 1.6$ and $\Lambda = 0.74$ GeV. We provide a comparison with experimental measurements extracted from [46]. Both resonances (ρ and ϕ) are reproduced in our calculation.

5. Conclusion

In this work, we have presented the calculation of the charged pion and kaon electromagnetic form factors in the time-like regime using the non-perturbative formalism of SDEs and BSEs. To accurately represent experimental data for a time-like photon, we have incorporated explicit mesonic contributions into the coupled SDE/BSE system, in addition to the Rainbow-Ladder truncation. The new diagrams facilitate the decay mechanisms of $\rho \to \pi\pi$ and $\phi \to KK$ in the QPV, which consequently impacts the form factors, as evidenced by the presented plots.

The main approximation used in these calculations involves the IA when calculating the form factor and a minor violation of the AxWTI. The resonance poles extracted from our results for the ρ and ϕ are in close proximity to the experimental values. It is crucial to emphasize that our calculations were conducted under the isospin symmetric limit, meaning that mixing effects such as $\omega - \rho$ are not incorporated in the formalism. The exploration of isospin symmetry breaking effects in the form factors is planned for future investigations.

Acknowledgments

A. S. Miramontes acknowledges *Consejo Nacional de Ciencia y Teconología* (CONACyT), Mexico, for the financial support provided to him through the program "*Postdoctorados Nacionales por México*". The work of A. Bashir is supported in part by the US Department of Energy (DOE) Contract No. DE-AC05-06OR23177, under which Jefferson Science Associates, LLC operates Jefferson Lab. A. Bashir also acknowledges Coordinación de la Investigación Científica of the Universidad Michoacana de San Nicolás de Hidalgo grant 4.10 and the Fulbright-García Robles scholarship for his stay as a visiting scientist at the Thomas Jefferson National Accelerator Facility, Newport News, Virginia, USA.

We dedicate this work to the fond memories of our colleague and fellow researcher Axel Weber.

1. R. R. Akhmetshin *et al*., High-statistics measurement of the pion form factor in the ρ-meson energy range with the CMD- 2 detector, *Phys. Lett. B* **648** (2007) 28, https://doi.org/10.1016/j.physletb.2007.01.073.
2. V. M. Aul'chenko *et al*., Measurement of the pion form-factor in the range 1.04-1.38-GeV with the CMD-2 detector, *JETP Lett.* **82** (2005) 743, https://doi.org/10.1134/1.2175241.
3. L. Barkov *et al*., Electromagnetic Pion Form-Factor in the Timelike Region, *Nucl. Phys. B* **256** (1985) 365, https://doi.org/10.1016/0550-3213(85)90399-2.
4. D. Bisello *et al*., The Pion Electromagnetic Form-factor in the Timelike Energy Range $1.35 \leq \sqrt{s} \geq 2.4$-GeV, *Phys. Lett. B* **220** (1989) 321, https://doi.org/10.1016/0370-2693(89)90060-9.
5. C. N. Brown *et al.*, Coincidence electroproduction of charged pions and the pion form-factor, *Phys. Rev. D* **8** (1973) 92, https://doi.org/10.1103/PhysRevD.8.92.
6. C. J. Bebek *et al.*, Further measurements of forward-chargedpion electroproduction at large κ^2, *Phys. Rev. D* **9** (1974) 1229, https://doi.org/10.1103/PhysRevD.9.1229.
7. T. Horn *et al.*, Determination of the Charged Pion Form Factor at $Q^{**2} = 1.60$ and 2.45 (GeV/c)^{**2}, *Phys. Rev. Lett.* **97** (2006) 192001, https://doi.org/10.1103/PhysRevLett.97.192001.
8. C. J. Bebek *et al*., Measurement of the pion form-factor up to $q^2 = 4$-GeV^2, *Phys. Rev. D* **13** (1976) 25, https://doi.org/10.1103/PhysRevD.13.25.
9. S. R. Amendolia *et al.*, A Measurement of the Kaon Charge Radius, *Phys. Lett. B* **178** (1986) 435, https://doi.org/10.1016/0370-2693(86)91407-3.
10. E. B. Dally *et al*., Direct measurement of the negative kaon form-factor, *Phys. Rev. Lett.* **45** (1980) 232, https://doi.org/10.1103/PhysRevLett.45.232.
11. C. J. Shultz, J. J. Dudek, and R. G. Edwards, Excited meson radiative transitions from lattice QCD using variationally optimized operators, *Phys. Rev. D* **91** (2015) 114501, https://doi.org/10.1103/PhysRevD.91.114501.
12. X. Gao *et al*., Pion form factor and charge radius from lattice QCD at the physical point, *Phys. Rev. D* **104** (2021) 114515, https://doi.org/10.1103/PhysRevD.104.114515.
13. P. Maris and P. C. Tandy, The π, K^+, and K^0 electromagnetic form-factors, *Phys. Rev. C* **62** (2000) 055204, https://doi.org/10.1103/PhysRevC.62.055204.
14. L. Chang *et al*., Pion electromagnetic form factor at spacelike momenta, *Phys. Rev. Lett.* **111** (2013) 141802, https://doi.org/10.1103/PhysRevLett.111.141802.
15. H. J. Kwee and R. F. Lebed, Pion form-factors in holographic QCD, *JHEP* **01** (2008) 027, https://doi.org/10.1088/1126-6708/2008/01/027.
16. J. Bijnens and P. Talavera, Pion and kaon electromagnetic form-factors, *JHEP* **03** (2002) 046, https://dx.doi.org/10.1088/1126-6708/2002/03/046.
17. Z. Abidin and P. T. P. Hutauruk, Kaon form factor in holographic QCD, *Phys. Rev. D* **100** (2019) 054026, https://doi.org/10.1103/PhysRevD.100.054026.
18. C. Burden, C. Roberts, and M. Thomson, Electromagnetic form-factors of charged and neutral kaons, *Phys. Lett. B* **371** (1996) 163, https://doi.org/10.1016/0370-2693(96)00006-8.
19. X. Wang *et al*., Pion scalar, vector and tensor form factors from a contact interaction *Phys. Rev. D* **106** (2022) 054016, https://link.aps.org/doi/10.1103/PhysRevD.106.054016.

20. A. Miramontes *et al.*, Pion and Kaon box contribution to $a\hat{I}\frac{1}{4}$HLbL, *Phys. Rev. D* **105** (2022) 074013, https://doi.org/10.1103/PhysRevD.105.074013.
21. L. Albino *et al*., Pseudoscalar mesons: Light front wave functions, GPDs, and PDFs, *Phys. Rev. D* **106** (2022) 034003, https://doi.org/10.1103/PhysRevD.106.034003.
22. R. J. Hernández-Pinto *et al*., Electromagnetic Form Factors and Charge Radii of Pseudoscalar and Scalar Mesons: A Comprehensive Contact Interaction Analysis, *Phys. Rev. D* **107** (2023) 054002, https://link.aps.org/doi/10.1103/PhysRevD.107.054002.
23. D. Stamen *et al*., Kaon electromagnetic form factors in dispersion theory, *Eur. Phys. J. C* **82** (2022) 432, https://doi.org/10.1140/epjc/s10052-022-10348-3.
24. D. Melikhov, O. Nachtmann, and T. Paulus, The Pion form-factor at time - like momentum transfers in a dispersion approach (2002). https://doi.org/10.48550/arXiv.hep-ph/0209151.
25. C. Bruch, A. Khodjamirian, and J. H. Kuhn, Modeling the pion and kaon form factors in the timelike region, *Eur. Phys. J. C* **39** (2005) 41, https://doi.org/10.1140/epjc/s2004-02064-3.
26. X. Feng *et al*., Timelike pion form factor in lattice QCD, *Phys. Rev. D* **91** (2015) 054504, https://doi.org/10.1103/PhysRevD.91.054504.
27. A. S. Miramontes, H. Sanchis Alepuz, and R. Alkofer, Elucidating the effect of intermediate resonances in the quark interaction kernel on the timelike electromagnetic pion form factor, *Phys. Rev. D* **103** (2021) 116006, https://doi.org/10.1103/PhysRevD.103.116006.
28. A. S. Miramontes and A. Bashir, Timelike electromagnetic kaon form factor, *Phys. Rev. D* **107** (2023) 014016, https://doi.org/10.1103/PhysRevD.107.014016.
29. D. Nicmorus, G. Eichmann, and R. Alkofer, Delta and Omega electromagnetic form factors in a Dyson-Schwinger/Bethe-Salpeter approach, *Phys. Rev. D* **82** (2010) 114017, https://doi.org/10.1103/PhysRevD.82.114017.
30. G. Eichmann and C. S. Fischer, Nucleon axial and pseudoscalar form factors from the covariant Faddeev equation, *Eur. Phys. J. A* **48** (2012) 9, https://doi.org/10.1140/epja/i2012-12009-6.
31. H. Sanchis-Alepuz, R. Alkofer, and C. S. Fischer, Electromagnetic transition form factors of baryons in the space-like momentum region, *Eur. Phys. J. A* **54** (2018) 41, https://doi.org/10.1140/epja/i2018-12465-x.
32. K. Raya *et al.*, Structure of the neutral pion and its electromagnetic transition form factor, *Phys. Rev. D* **93** (2016) 074017, https://doi.org/10.1103/PhysRevD.93.074017.
33. I. C. Cloët and C. D. Roberts, Explanation and Prediction of Observables using Continuum Strong QCD, *Prog. Part. Nucl. Phys.* **77** (2014) 1, https://doi.org/10.1016/j.ppnp.2014.02.001.
34. B. El-Bennich *et al.*, Excited hadrons and the analytical structure of bound-state interaction kernels, *Few Body Syst.* **57** (2016) 955, https://doi.org/10.1007/s00601-016-1133-x.
35. A. S. Miramontes *et al*., Electromagnetic and strong isospin breaking in light meson masses, *Phys. Lett. B* **833** (2022) 137291, https://doi.org/10.1016/j.physletb.2022.137291.
36. G. Eichmann *et al*., Baryons as relativistic three-quark bound states, *Prog. Part. Nucl. Phys.* **91** (2016) 1, https://doi.org/10.1016/j.ppnp.2016.07.001.
37. A. Bashir *et al*., Collective perspective on advances in Dyson-Schwinger Equation QCD, *Commun. Theor. Phys.* **58** (2012) 79, https://doi.org/10.1088/0253-6102/58/1/16.
38. A. S. Miramontes and H. Sanchis-Alepuz, On the effect of resonances in the quark-photon vertex, *Eur. Phys. J. A* **55** (2019) 170, https://doi.org/10.1140/epja/i2019-12847-6.
39. C. S. Fischer, D. Nickel, and J.Wambach, Hadronic unquenching effects in the quark propagator, *Phys. Rev. D* **76** (2007) 094009, https://doi.org/10.1103/PhysRevD.76.094009.
40. C. S. Fischer, D. Nickel, and R. Williams, On Gribov's supercriticality picture of quark confinement, *Eur. Phys. J. C* **60** (2009) 47, https://doi.org/10.1140/epjc/s10052-008-0821-1.
41. H. Sanchis-Alepuz, C. S. Fischer, and S. Kubrak, Pion cloud effects on baryon masses, *Phys. Lett. B* **733** (2014) 151, https://doi.org/10.1016/j.physletb.2014.04.031.
42. R. Williams, Vector mesons as dynamical resonances in the Bethe-Salpeter framework, *Phys. Lett. B* **798** (2019) 134943, https://doi.org/10.1016/j.physletb.2019.134943.
43. P. D. Group, Review of Particle Physics, *Progress of Theoretical and Experimental Physics* **2022** (2022), https://doi.org/10.1093/ptep/ptac097.
44. R. Alkofer, A. S. Miramontes, and H. Sanchis-Alepuz, Elucidating the ρ-meson's role as intermediate resonance in the time-like electromagnetic pion form factor, *EPJWeb Conf.* **262** (2022) 01020, https://doi.org/10.1051/epjconf/202226201020.
45. F. V. Ignatov *et al*., Measurement of the $e^+e^- \to \pi^+\pi^-$ cross section from threshold to 1.2 GeV with the CMD-3 detector (2023), https://doi.org/10.48550/arXiv.2302.08834.
46. E. A. Kozyrev *et al*., Study of the process $e^+e^- \to K^+K^-$ in the center-of-mass energy range 1010-1060 MeV with the CMD-3 detector, *Phys. Lett. B* **779** (2018) 64, https://doi.org/10.1016/j.physletb.2018.01.079.